Curcumin and Dehydrozingerone Derivatives: Synthesis, Radiolabeling, and Evaluation for β-Amyloid Plaque Imaging[†]

Eun Kyoung Ryu, Yearn Seong Choe,* Kyung-Han Lee, Yong Choi, and Byung-Tae Kim

Department of Nuclear Medicine, Samsung Medical Center, Sungkyunkwan University School of Medicine, 50 Ilwon-dong, Kangnam-ku, Seoul 135-710, Korea

Alzheimer's disease (AD) is pathologically characterized by the accumulation of amyloid plaques and neurofibrillary tangles in the brain, and thus, the in vivo imaging of plaques and tangles would be beneficial for the early diagnosis of AD. It has been suggested that 5-hydroxy-1,7-bis(4-hydroxy-3-methoxyphenyl)-1,4,6-heptatrien-3-one (curcumin) may be responsible for low age-adjusted prevalence of AD in India. In the present study, eight novel derivatives of curcumin and 4-(4-hydroxy-3-methoxyphenyl)-3-buten-2-one (dehydrozingerone) were synthesized and their binding affinities for β-amyloid (Aβ) aggregates were measured. Of these ligands, fluoropropyl-substituted curcumin (**8**) showed the highest binding affinity (K_i = 0.07 nM), and therefore, **8** was radiolabeled and evaluated as a potential probe for Aβ plaque imaging. Partition coefficient measurement and biodistribution in normal mice demonstrated that [^{18}F]**8** has a suitable lipophilicity and reasonable initial brain uptake. Metabolism studies also indicated that [^{18}F]**8** is metabolically stable in the brain. These results suggest that [^{18}F]**8** is a suitable radioligand for Aβ plaque imaging.

Introduction

Alzheimer's disease (AD)[a] is a progressive neurodegenerative disorder and a leading cause of dementia. AD is characterized by abundant senile plaques composed of Aβ peptides and numerous neurofibrillary tangles formed from filaments of highly phosphorylated tau proteins, which are invariably observed in the postmortem brain tissues of AD patients.[1−3] Therefore, the monitoring of Aβ plaques and neurofibrillary tangles may be beneficial for the diagnosis, staging, and treatment of AD.

Many specific ligands have been developed for the imaging of Aβ plaques. These are based on fluorescent dyes that are used to stain Aβ plaques and neurofibrillary tangles in vitro and include highly conjugated symmetric compounds, such as Congo red (CR) and chrysamine-G (CG), and a smaller molecule, such as thioflavin-T (Figure 1).[4] However, radioiodine-labeled CR has low brain uptake, probably because of the hydrophilic nature of its sulfonate groups.[5] The more lipophilic CG has been labeled with ^{125}I or ^{99m}Tc−monoamine−monoamide bisthiol (MAMA), but studies showed low brain uptake in rodents.[6−8] Lansbury and co-workers synthesized the positively charged ^{99m}Tc(bipyridyl)(*t*-butylisonitrile)$_4$ derivatives of CR and CG, and found that they had K_d values for Aβ(1−40) comparable to those of CR for insulin amyloid fibrils and of CG for Aβ(10−43).[9] This group further prepared neutral Re-(=O)−MAMA−CR and CG complexes and a Tc(=O)−MAMA−CR complex. The Re complexes showed affinities for Aβ(40) comparable to those of CR and CG and stained amyloid plaques in AD brain sections.[10] However, the complexes may exceed the physicochemical and molecular weight limitations (700 Daltons) imposed by the blood−brain barrier (BBB).[4,11,12] In other studies, CG was further modified to increase brain

uptake; diazo groups and a biphenyl group were replaced by vinyl groups and a phenyl group, respectively, in 1,4-bis(3-hydroxycarbonyl-4-hydroxyphenylethenyl)benzene (X-34, K_i = 17.8 nM),[4,13] 1-bromo-2,5-bis(3-hydroxycarbonyl-4-hydroxy)-styrylbenzene (BSB, K_i = 400 nM),[14] 1-iodo-2,5-bis(3-hydroxy-carbonyl-4-hydroxy)styrylbenzene (ISB, K_d = 0.08 nM), and 1-iodo-2,5-bis(3-hydroxycarbonyl-4-methoxy)styrylbenzene (IM-SB, K_i = 0.17 nM; Figure 1).[15] Radioiodine-labeled ISB and IMSB showed lower initial brain uptakes in normal mice (0.27% ID/organ and 0.14% ID/organ at 5 min after injection) than radioiodinated thioflavin-T derivatives (0.6−3.5% ID/organ at 2 min),[15] despite their potent binding affinities for Aβ aggregates.[15] This may be because that the carboxylic acids of CG derivatives would be mostly ionized in the physiological pH range, which would reduce their abilities to cross the BBB.

A neutral and lipophilic fluorescent dye, 2-(1-{6-[dimethyl-amino]-2-naphthyl}ethylidene)malononitrile (DDNP) was also modified for ^{18}F labeling. A fluoromethyl derivative of DDNP (FDDNP) was found to have a K_d of 0.12 nM for high binding sites on Aβ aggregates and a K_d of 1.86 nM for low binding sites. [^{18}F]FDDNP was found to easily traverse the BBB due to its high lipophilicity (log P = 3.92). This radioligand was found to label both senile plaques and neurofibrillary tangles in the brains of AD patients with positron emission tomography (PET).[16,17]

A charged molecule, thioflavin-T, was structurally modified to improve its brain permeability;[4,18,19] the neutral benzothiazole derivatives obtained include 2-[4′-(dimethylamino)phenyl]-6-iodobenzothiazole (TZDM, K_i = 1.9 nM),[15] 2-(4′-dimethylami-nophenyl)-6-iodobenzoxazole (IBOX, K_i = 0.8 nM),[20] 6-iodo-2-(4′-(dimethylamino)-)phenyl-imidazo[1,2-*a*]pyridine (IMPY, K_i = 15 nM),[21] and 2-(4′-(methylamino)phenyl-6-hydroxyben-zothiazole (6-OH−BTA-1, K_i = 4.3 nM; Figure 1),[22] However, although [^{125}I]TZDM and [^{125}I]IBOX labeled Aβ in postmortem AD brain sections, they showed slow washout from normal mouse brain.[15,20] Radioiodine-labeled benzofuran derivatives also showed slow radioactivity washout from normal mouse brain, indicating a high level of nonspecific binding in vivo.[23] However, [^{125}I]IMPY showed good initial brain uptake (2.88%

* Corresponding author. Tel.: +82-2-3410-2623. Fax: +82-2-3410-2639. E-mail: ysnm.choe@samsung.com.
[a] Abbreviations: AD, Alzheimer's disease; Aβ, β-amyloid; BBB, blood−brain barrier; PET, positron emission tomography; SPECT, single photon emission computed tomography.
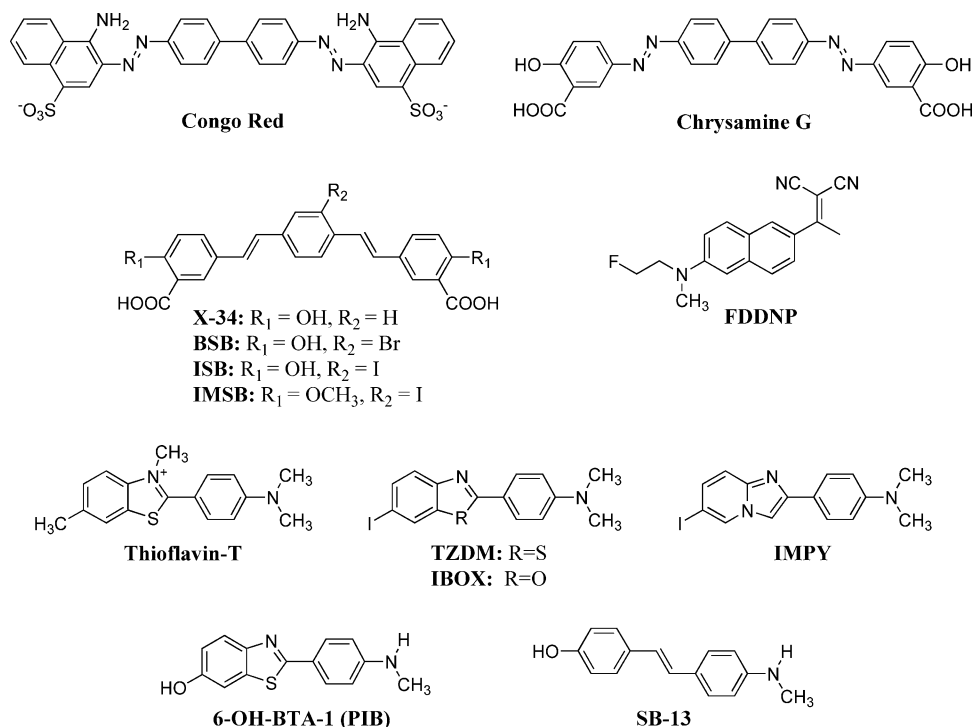
Figure 1. Chemical structures of CR, CG, styrylbenzene derivatives, FDDNP, thioflavin-T derivatives, and stilbene derivative.

ID/organ at 2 min) and rapid washout from normal mouse brain,[21] and labeled regions containing Aβ in transgenic PSAPP mouse brain sections and also in postmortem AD brain sections.[24,25] [^{11}C]6-OH–BTA-1 (PIB), a benzothiazole–aniline derivative, was also found to have high initial uptake and rapid clearance from normal mouse and baboon brains,[22] and human trials with this radioligand showed high uptake in brains of AD patients and significant retention in frontal and temporoparietal cortex, the anterior and posterior cingulated cortex, and the striatum, which is consistent with the known pattern of Aβ plaque distribution in the AD brain.[4,26,27]

Stilbene derivatives were also found to have good binding affinities for Aβ aggregates in vitro (K_i = 1.2–151 nM). In particular, ^{11}C-labeled 4-*N*-methylamino-4′-hydroxystilbene (SB-13 (Figure 1), K_i = 6.0 nM) displayed moderate lipophilicity (log *P* = 2.36), high initial brain uptake in the normal rat cortex (1.51% ID/g at 2 min), and rapid washout (0.42% ID/g at 30 min). This radioligand also showed specific labeling of Aβ plaques in brain sections from transgenic (TgCRDN8) mice.[28]

5-Hydroxy-1,7-bis(4-hydroxy-3-methoxyphenyl)-1,4,6-heptatrien-3-one (curcumin) has been extensively studied for its anticancer, antioxidant, and anti-inflammatory activities.[29–31] Moreover, it has also been reported that the age-adjusted prevalence of AD patients in India is 4.4-fold less than that in the U.S.A.,[32] and it was suggested that this may be explained by the fact that curcumin, a major ingredient of the curry spice turmeric, is used as a food preservative and herbal medicine in India.[33] Moreover, it has a favorable toxicity profile in mice and was found to cause no adverse effects in cancer patients during clinical studies.[29,33] In addition, curcumin has been reported to have favorable brain permeability, and satisfactory Aβ plaque binding properties have been predicted from the fluorescence staining of Aβ plaques in brain sections from APPsw transgenic mice administered curcumin by injection or in diet.[34] 4-(4-Hydroxy-3-methoxyphenyl)-3-buten-2-one (dehydrozingerone), a partial structure of curcumin, is also known to have antioxidant properties.[35]

Scheme 1[a]
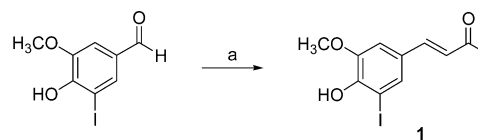
[a] Reagents and conditions: (a) acetone, 2.5 M NaOH, rt, 24 h, 54%.

In the present study, curcumin and dehydrozingerone derivatives were synthesized and evaluated in vitro and in vivo as Aβ plaque imaging probes for PET or single photon emission computed tomography (SPECT).

Results and Discussion

Chemistry. The syntheses of dehydrozingerone and curcumin derivatives are shown in Schemes 1–4. Dehydrozingerone derivatives, **1**–**3**, were prepared by aldol condensations of the vanillin derivatives and acetone in the presence of 2.5 M NaOH (Schemes 1 and 2).[36] Recrystallization from ethanol and water yielded orange-colored products. Fluoroalkyl derivatives of dehydrozingerone, **2** and **3**, were prepared as in Scheme 2. Compounds **9** and **10** were prepared in high yields from the *O*-alkylation of vanillin with the corresponding dibromoalkanes in the presence of K$_2$CO$_3$. The bromo groups of **9** and **10** were converted into tosyl groups, as in **11** and **12**, using silver *p*-toluenesulfonate under reflux overnight, and these were further substituted with fluorine atoms using *n*-Bu$_4$NF to give **13** and **14**. Aldol condensation of the resulting aldehyde and acetone, followed by dehydration, afforded the dehydrozingerone derivatives **2** and **3**.

Aldol condensation of acetylacetone–boron complex and vanillin derivatives is a key step in acetylation of the dehydrozingerone in ligands **4**–**6**.[37] Keto-enol compounds (**4**, **5**, **6**, **15**, and **16**) were synthesized by reacting the corresponding aldehydes with 2 equiv of acetylacetone–boron complex. Recrystallization from ethanol and water gave products that were visualized by fluorescence and UV illumination.

Curcumin derivatives, **7**, **8**, and **17** were synthesized by coupling keto-enol compounds and the corresponding vanillin

Scheme 2[a]
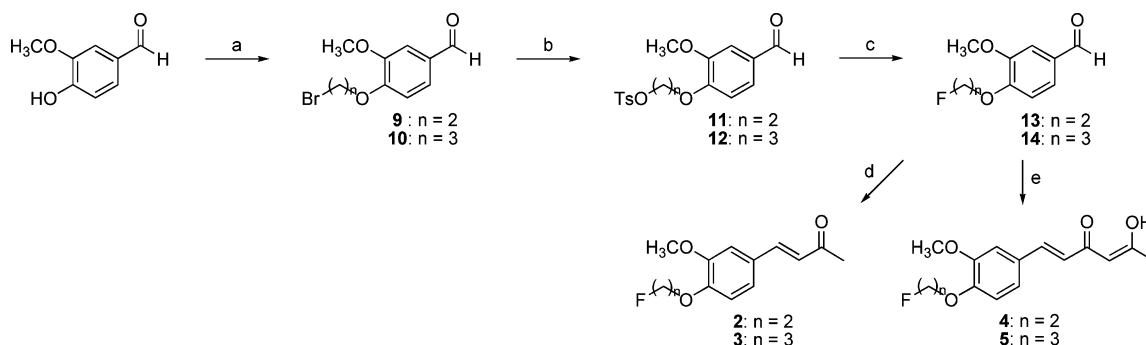
[a] Reagents and conditions: (a) Br(CH₂)ₙBr, K₂CO₃, DMF, 80 °C, 1 h, 65−99%; (b) AgOTs, CH₃CN, reflux, overnight, 66−85%; (c) *n*-Bu₄NF, THF, reflux, 4 h, 74−91%; (d) acetone, 2.5 M NaOH, rt, 24 h, 68−83%; (e) 2,4-pentanedione, B₂O₃, (*n*-BuO)₃B, ethyl acetate, 80 °C, 30 min, *n*-BuNH₂, 100 °C, 30 min, 1 N HCl, 50 °C, 30 min, 48−53%.

Scheme 3[a]
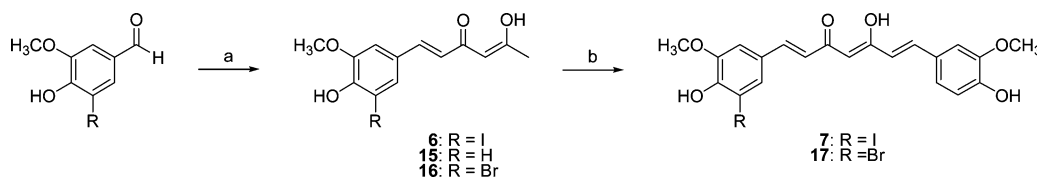
[a] Reagents and conditions: (a) 2,4-pentanedione, B₂O₃, (*n*-BuO)₃B, ethyl acetate, 80 °C, 30 min, *n*-BuNH₂, 100 °C; 30 min, 1 N HCl, 50 °C, 30 min, 59−85%; (b) vanillin, B₂O₃, (*n*-BuO)₃B, ethyl acetate, 80 °C, piperidine, 80 °C, 30 min, 0.4 N HCl, 50 °C, 30 min, 50−58%.

Scheme 4[a]
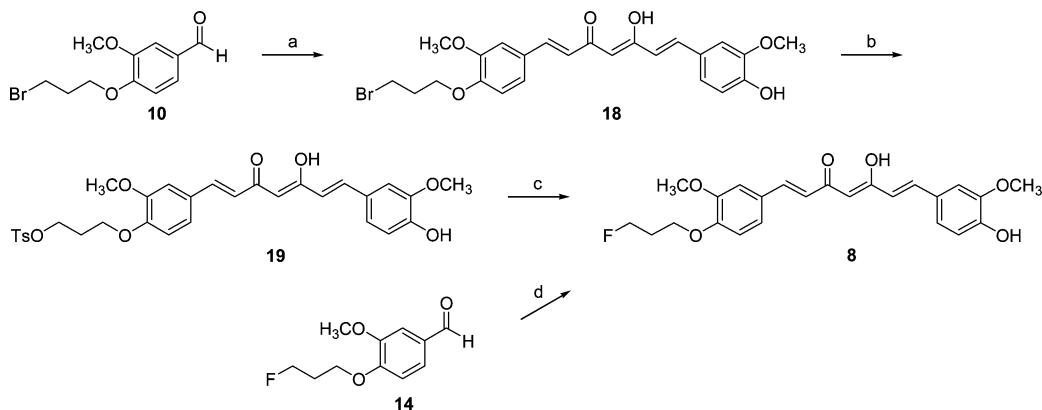
[a] Reagents and conditions: (a) **15**, B₂O₃, (*n*-BuO)₃B, ethyl acetate, 80 °C, piperidine, 80 °C, 30 min, 0.4 N HCl, 50 °C, 30 min, 37.6%; (b) AgOTs, CH₃CN, reflux, overnight, 62%; (c) *n*-Bu₄NF, THF, reflux, 4 h, 23%; (d) **15**, B₂O₃, (*n*-BuO)₃B, ethyl acetate, 80 °C, piperidine, 80 °C, 30 min, 0.4 N HCl, 50 °C, 30 min, 54%.

derivative−boron complexes in the presence of piperidine, which was found to give better yields than when *n*-butylamine was used (Schemes 3 and 4).[37] Direct iodination of curcumin to produce **7** yielded a side product that probably resulted from iodination at the C4 position. To prepare the radioligands ([¹²⁵I]-**6** and [¹²⁵I]**7**) with high specific activity, bromo compounds were used instead of iodo compounds to synthesize the precursors shown in Schemes 5 and 6. Bromo groups were converted to the tributylstannyl precursors, **20** and **21**, using bis(tributyltin) in the presence of Pd(PPh₃)₄.

The fluoropropyl derivative of curcumin was synthesized using two different methods, as shown in Scheme 4. The tosylate precursor **19** was prepared by coupling **10** and the **15**−boron complex, and this was followed by substituting the bromo group with a tosyl group. However, the subsequent substitution with *n*-Bu₄NF to give ligand **8** was only achieved in a yield of 23%. As an alternative pathway, the hydroxyl group of **18** was protected as an acetyl ester with acetic anhydride in pyridine in high yield, and this was followed by substitution of the bromo group with a tosyl group. However, fluorination of the tosylate

Scheme 5[a]
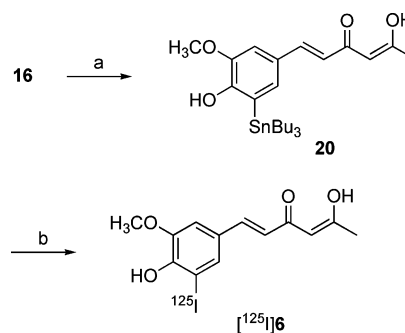
[a] Reagents and conditions: (a) Pd(PPh₃)₄, (SnBu₃)₂, toluene, 110 °C, overnight, 20%; (b) Na¹²⁵I, 1 N HCl, 3% H₂O₂, ethanol, rt, 10 min, 10−14%.

precursor also had a low yield (13%), and therefore, **14** was coupled with **15** to prepare the product **8** (32%).

Radiolabeling. [¹²⁵I]**6** and [¹²⁵I]**7** were prepared by radio-iododestannylation of the corresponding tributylstannyl precur-
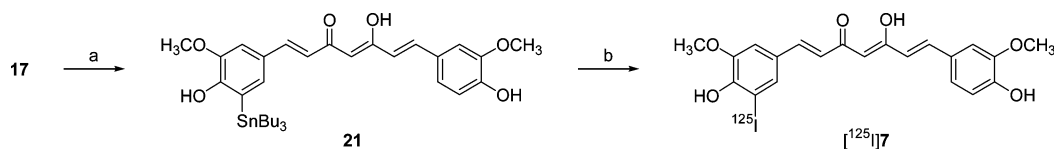
Scheme 6[a]

[a] Reagents and conditions: (a) Pd(PPh$_3$)$_4$, (SnBu$_3$)$_2$, toluene, 110 °C, overnight, 19%; (b) Na^{125}I, 1 N HCl, 3% H$_2$O$_2$, rt, 10 min, 35−40%.

Scheme 7[a]
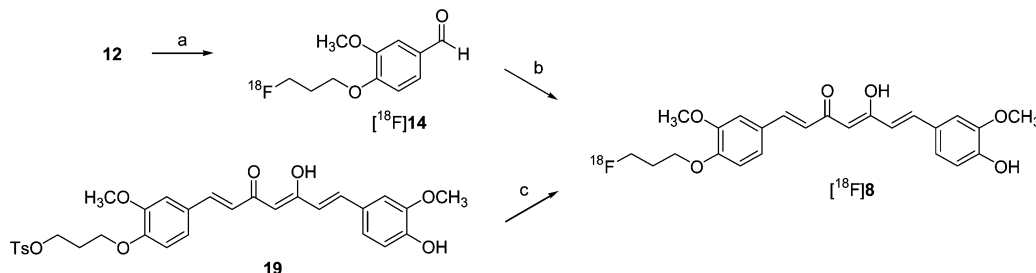
[a] Reagents and conditions: (a) n-Bu$_4$N^{18}F, CH$_3$CN, 105 °C, 10 min, >85%; (b) **15**, B$_2$O$_3$, (n-BuO)$_3$B, piperidine, ethyl acetate, 105 °C, 15 min, 0.4 N HCl, 90 °C, 5 min, 16−25%; (c) n-Bu$_4$N^{18}F, THF, 95 °C, 20 min, 0−17%.

sors, **20** and **21**, respectively, using Na[^{125}I]I in the presence of 3% H$_2$O$_2$ at room temperature for 10 min (Schemes 5 and 6). The reaction was quenched with saturated NaHSO$_3$, and the mixture was purified by HPLC. Decay-corrected radiochemical yields of [^{125}I]**6** and [^{125}I]**7** were 10−14% and 35−40% and specific activities were 72.6 GBq/μmol and 87.3 GBq/μmol, respectively.

Radioligand [^{18}F]**8** was synthesized as shown in Scheme 7. When precursor **19** was used for ^{18}F-labeling, [^{18}F]**8** was synthesized in variable yields (0−17%). As an alternative pathway, nucleophilic [^{18}F]fluorination of acetyl protected tosylate precursor also gave the product in low yield (13%) and with low effective specific activity. Therefore, [^{18}F]**14**, which was prepared from **12** and n-Bu$_4$N[^{18}F]F (>85%), was used for the preparation of [^{18}F]**8**. The subsequent aldol condensation with acetylacetone−boron complex, followed by HPLC purification, gave the product in overall decay-corrected radiochemical yield of 16−25% and with an effective specific activity of 37.6 GBq/μmol.

Binding Assays. In vitro binding assays using Aβ(1−40) aggregates were performed as described in the literature,[15,18] and radiolabeled standards, [^{125}I]IMSB and [^{125}I]IMPY, were prepared as previously described.[15,21] Their K_d values for binding to Aβ(1−40) aggregates were similar to those reported, that is, 0.18 nM versus 0.13 nM (reported) for [^{125}I]IMSB and 17.3 nM versus 5.4 nM (reported value obtained using the gray matter homogenates of AD brains) for [^{125}I]IMPY.[15,25] The binding affinities of ligands described here were determined using Aβ aggregates and the radiolabeled standards, [^{125}I]IMSB or [^{125}I]-IMPY, depending on the structures of the ligands tested, and nonspecific binding was measured in the presence of CG or thioflavin-T (Table 1). [^{125}I]IMSB and CG were used for curcumin derivatives, but [^{125}I]IMPY and thioflavin-T were used for dehydrozingerone derivatives.

Dehydrozingerone derivatives, including **1−6**, showed lower affinities for Aβ aggregates than curcumin derivatives. In particular, 2-fluoroalkyl ligands, **2−5**, exhibited K_i values higher than 200 nM for the Aβ aggregates. On the other hand, the iodine-substituted ligands, **1** and **6**, showed reasonable K_i values (36.6 nM and 24.9 nM, respectively) for Aβ aggregates. Dehydrozingerone was found to have similar affinities for Aβ aggregates upon using [^{125}I]IMPY or [^{125}I]IMSB (55.9 nM vs 54.2 nM, respectively) as the radiolabeled standards, and ligand

Table 1. K_i (nM) of Ligands for Aβ(1−40) Aggregates

| ligand	[^{125}I]IMPY	[^{125}I]IMSB
dehydrozingerone	55.9 ± 4.0	54.24
1	36.6 ± 1.2	19.97 ± 2.7
2	232.7 ± 16	
3	839.2	
4	958.1 ± 93	
5	316.3 ± 69	
6	24.9 ± 0.9	
CG		0.16 ± 0.04
curcumin		0.20 ± 0.06
7		9.37 ± 1.0
8		0.07 ± 0.01

1 competed better with [^{125}I]IMSB binding than [^{125}I]IMPY binding to Aβ aggregates (19.97 nM vs 36.6 nM).

CG showed a similar K_i value (0.16 nM) to that reported (0.14 nM) for binding to Aβ(1−40) aggregates.[15] Curcumin exhibited potent binding affinity for Aβ(1−40) aggregates (K_i = 0.20 nM), but the introduction of an iodine into its phenyl ring (**7**) significantly decreased its binding affinity by 47-fold, whereas O-fluoropropylation of its hydroxyl group (**8**) increased binding affinity 2.9-fold, giving a K_i value of 0.07 nM. These results demonstrate that a highly conjugated dimeric structure is required for high Aβ aggregate binding affinity.

Partition Coefficient Measurement. The partition coefficients of some ligands were measured using radiolabeled forms, that is, [^{125}I]**6**, [^{125}I]**7**, and [^{18}F]**8** had log $P_{o/w}$ values of 1.35, 0.94, and 1.84, respectively, predicting a favorable brain permeability for all three. Of these radioligands, [^{18}F]**8** is most preferable for in vivo evaluations because of its high binding affinity and suitable lipophilicity.

Metabolism Studies. Radioligand [^{18}F]**8** was analyzed using mouse brain and blood and remained intact in the brain during the time of the study (60 min), whereas an unidentified polar metabolite appeared in blood samples within 2 min after injection and [^{18}F]**8** was completely converted into the metabolite at 60 min (Figure 2). This polar radioactive metabolite did not seem to cross the BBB because of its high polarity. These results demonstrate that [^{18}F]**8** is metabolically stable in the mouse brain after being taken up.

Biodistribution. Radioligands ([^{125}I]**6** and [^{18}F]**8**) were evaluated in normal mice to assess their ability to cross the BBB. Radioligand [^{125}I]**6** showed a similar initial brain uptake (0.69% ID/g) to [^{18}F]**8**, but lower radioactivity accumulation in liver,
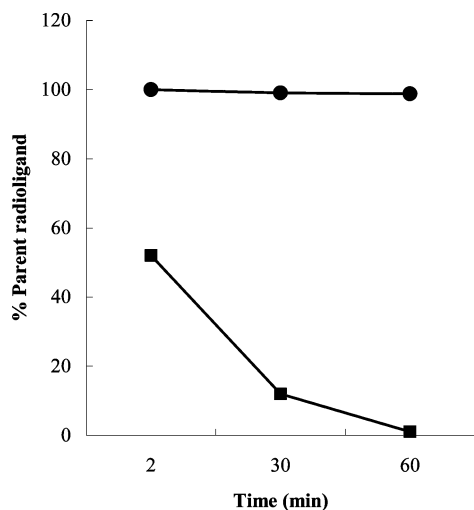
Figure 2. Metabolism of [^{18}F]**8** in mouse brain and blood. Data are presented as % parent radioligand in brain (●) and in blood (■) as determined by radio-TLC as a function of time (2, 30, and 60 min).

Table 2. Biodistribution of [^{125}I]**6** in Normal Mice

organ	2 min	30 min	60 min	120 min
blood	17.92 ± 7.65	2.05 ± 0.47	0.87 ± 0.05	0.64 ± 0.09
thyroid	4.60 ± 0.70	10.25 ± 1.44	23.18 ± 4.05	27.63 ± 13.0
heart	5.23 ± 0.87	0.72 ± 0.13	0.31 ± 0.02	0.20 ± 0.05
lung	14.78 ± 9.86	1.30 ± 0.35	0.57 ± 0.06	0.57 ± 0.20
liver	18.28 ± 0.60	4.64 ± 1.23	2.85 ± 0.51	2.53 ± 0.42
spleen	4.61 ± 1.31	1.93 ± 0.46	1.81 ± 0.44	1.37 ± 0.40
kidney	11.82 ± 1.37	9.63 ± 1.17	2.34 ± 0.34	1.03 ± 0.10
muscle	1.35 ± 0.13	0.54 ± 0.14	0.26 ± 0.07	0.13 ± 0.04
brain	0.69 ± 0.08	0.11 ± 0.05	0.05 ± 0.01	0.02 ± 0.01

spleen, and lungs (Table 2). The high thyroid uptake of [^{125}I]**6** indicated that this radioligand was deiodinated in vivo (4.6% ID/g at 2 min, 10.3% ID/g at 30 min, and 23.2% ID/g at 60 min).

Biodistribution studies on [^{18}F]**8** demonstrated that high and persistent radioactivity accumulation occurred in the liver and spleen and that its lung uptake decreased with time. Brain uptake of [^{18}F]**8** was 0.52% ID/g at 2 min postinjection, and its radioactivity was rapidly washed out from the brain at 30 min (0.11% ID/g) (Table 3A). In addition, [^{18}F]**8** did not appear to undergo metabolic defluorination due to a constant level of bone uptake with time (2.7−3.4% ID/g). However, despite its suitable lipophilicity and reasonable molecular size (mol wt 428.45), its initial brain uptake was relatively low, which may be explained by its rapid metabolism in the liver and in the intestinal wall, like curcumin.[38] Piperine, a major component of black pepper, is a known inhibitor of hepatic and intestinal glucuronidation and is also shown to increase the bioavailability of curcumin. This effect of piperine on the pharmacokinetics of curcumin has been shown to be much greater in humans than in rats; in humans, curcumin bioavailability was increased by 2000% at 45 min after co-administering curcumin orally with piperine, whereas in rats, curcumin bioavailability was increased by only 154% between 1 and 2 h after co-administration.[38] Therefore, the effect of piperine on the uptake of [^{18}F]**8** was assessed after co-injecting [^{18}F]**8** with piperine. As shown in Table 3B, initial brain uptake (0.77% ID/g at 2 min) was increased by 48% (*p* value < 0.05) relative to that without piperine, although other organ uptakes were similar to those without piperine (Table 3A,B). However, the effect of piperine was limited, possibly due to its poor solubility in 10% ethanol−saline. Therefore, the initial brain uptake of [^{18}F]**8** would be

Table 3. Biodistribution of [^{18}F]**8** (A) and of [^{18}F]**8** Co-Injected with Piperine (B) in Normal Mice

(A)			
organ	2 min	30 min	60 min
blood	7.34 ± 1.29	1.24 ± 0.01	0.61 ± 0.45
heart	4.05 ± 0.40	0.57 ± 0.08	0.64 ± 0.08
lung	30.91 ± 4.43	7.23 ± 0.34	10.55 ± 1.73
liver	38.99 ± 2.80	41.06 ± 5.41	37.06 ± 6.24
spleen	16.32 ± 1.99	42.94 ± 1.19	36.05 ± 9.45
kidney	8.64 ± 0.35	2.71 ± 1.11	2.07 ± 0.58
muscle	0.89 ± 0.12	0.28 ± 0.16	0.27 ± 0.09
bone	3.23 ± 0.29	2.68 ± 0.11	3.43 ± 0.48
brain	0.52 ± 0.08	0.11 ± 0.03	0.11 ± 0.02

(B)			
organ	2 min	30 min	60 min	120 min
blood	11.18 ± 3.41	0.90 ± 0.05	0.82 ± 0.11	0.75 ± 0.16
heart	5.24 ± 1.10	0.70 ± 0.06	0.57 ± 0.03	0.38 ± 0.08
lung	34.26 ± 6.81	13.61 ± 1.33	7.88 ± 0.62	3.48 ± 1.26
liver	35.39 ± 3.93	43.13 ± 4.97	37.02 ± 4.77	18.53 ± 7.85
spleen	28.68 ± 7.26	36.25 ± 8.36	41.07 ± 1.66	21.49 ± 15.0
kidney	8.69 ± 1.04	2.81 ± 0.73	1.70 ± 0.41	0.99 ± 0.22
muscle	1.12 ± 0.18	0.36 ± 0.07	0.28 ± 0.03	0.20 ± 0.12
brain	0.77 ± 0.10	0.14 ± 0.02	0.09 ± 0.02	0.07 ± 0.02

significantly increased if the solubility of piperine can be enhanced in an injection solution.

An initial brain uptake higher than 0.5% ID/organ at 2 min after injection is preferred for Aβ plaque imaging probes, and this initial uptake should remain at less than 30% at 30 min in normal mouse brain because of the absence of Aβ plaques.[21,24] Although the initial brain uptakes of [^{125}I]**6** and [^{18}F]**8** fall slightly short of these criteria (0.24−0.34% ID/organ at 2 min), these radioligands showed rapid washout at 30 min. Thus, taken together with other in vitro and in vivo results, [^{125}I]**6** may be unsuitable for Aβ plaque imaging because of its severe in vivo deiodination. In contrast, [^{18}F]**8** has promise as an Aβ plaque imaging probe because it is metabolically stable in the brain and, therefore, it would strongly bind to Aβ plaques due to its excellent in vitro binding affinity (K_i = 0.07 nM) once taken up by the brain. Moreover, the fluorescence of curcumin derivatives aids locating Aβ plaques in vitro and, thus, offers an additional advantage.

Conclusion

Eight novel curcumin and dehydrozingerone derivatives were synthesized and evaluated in vitro and in vivo. The curcumin derivatives showed higher binding affinities for Aβ(1−40) aggregates than dehydrozingerone derivatives, with **8** being the most potent ligand. Moreover, [^{18}F]**8** showed suitable lipophilicity, reasonable initial brain uptake, and metabolic stability in the normal mouse brain. These results suggest that [^{18}F]**8** is a promising candidate for Aβ plaque imaging.

Experimental Section

Chemicals were purchased from Sigma-Aldrich (St. Louis, MO) and CG from Merck Biosciences (San Diego, CA). Aβ(1−40) peptide was obtained from Biosource, Inc. (Camarillo, CA), and Na[^{125}I]I from PerkinElmer Life and Analytical Sciences (Boston, MA). Dehydrozingerone and curcumin were synthesized as described in the literature.[36,37] ^{1}H NMR spectra were obtained using a Varian ^{Unity}*Inova* 500NB (500 MHz) spectrometer (Palo Alto, CA), and chemical shifts (δ) were reported in ppm downfield from tetramethylsilane. Electron impact (EI) and fast atom bombardment (FAB) mass spectra were obtained using a JMS-700 Mstation instrument (JEOL, Ltd., Tokyo, Japan). Elemental analysis was performed on a Flash EA 1112 (ThermoQuest CE Instruments, Milan, Italy). Purification of radioligand was carried out on a HPLC

(Thermo Separation Products System, Fremont, CA) equipped with a semipreparative column (YMC-Pack C18, 5 μ, 10 × 250 mm), and eluant was simultaneously monitored using a UV detector (254 nm) and a NaI(T1) radioactivity detector. Radio-thin-layer chromatography (TLC) was performed on Merck F_{254} silica plates and analyzed using a Bioscan scanner (Washington DC, U.S.A.).

[^{18}F]Fluoride was produced using the ^{18}O(p,n)^{18}F reaction on a PETtrace cyclotron (GE Healthcare, Uppsala, Sweden). Radioactivity was measured in a dose calibrator (Biodex Medical Systems, Shirley, NY), and tissue radioactivity was measured in a Wallac automated gamma counter (Boston, MA). All animal experiments complied with the rules of the Samsung Medical Center Laboratory Animal Care, which are based on NIH guidelines.

4-(2-Bromoethoxy)- and 4-(3-Bromopropoxy)-3-methoxybenzaldehyde (9 and 10). Vanillin (0.5 g, 3.29 mmol) and K_2CO_3 (0.64 g, 4.6 mmol) were added to 1,2-dibromoethane or 1,3-dibromopropane (9.79 mmol) in DMF (20 mL). The reaction mixture was then stirred at 80 °C for 1 h, cooled to 0 °C on an ice bath, quenched with 1 N HCl, and extracted with ethyl acetate. The organic layer was washed with water and dried over Na_2SO_4. Flash column chromatography (2:1 hexanes−ethyl acetate) afforded **9** (550 mg, 65%) or **10** (890 mg, 99%) as white solids.

4-(2-Bromoethoxy)-3-methoxybenzaldehyde (9): mp 71.4−72.1 °C; ^{1}H NMR (CDCl$_3$) δ 3.71 (t, J = 7.0 Hz, 2H), 3.96 (d, J = 5.0 Hz, 3H), 4.43 (t, J = 7.0 Hz, 2H), 7.00 (d, J = 8.5 Hz, 1H), 7.46 (dd, J = 5.8, 2.0 Hz, 2H), 9.89 (s, 1H); MS (EI) m/z 260 (M$^+$, ^{81}Br), 258 (M$^+$, ^{79}Br); HRMS calcd for C$_{10}$H$_{11}$^{81}BrO$_3$, 259.9872; found, 259.9875.

4-(3-Bromopropoxy)-3-methoxybenzaldehyde (10): mp 58.4−59.9 °C; ^{1}H NMR (CDCl$_3$) δ 2.39−2.44 (m, 2H), 3.64 (t, J = 6.5 Hz, 2H), 3.92 (s, 3H), 4.25 (t, J = 6.0 Hz, 2H), 7.01 (d, J = 8.0 Hz, 1H), 7.42−7.46 (m, 2H), 9.86 (s, 1H); MS (EI) m/z 274 (M$^+$, ^{81}Br), 272 (M$^+$, ^{79}Br); HRMS calcd for C$_{11}$H$_{13}$^{81}BrO$_3$, 274.0029; found, 274.0006. Anal. (C$_{11}$H$_{13}$BrO$_3$) C, H.

4-(2-Tosyloxyethoxy)- and 4-(3-Tosyloxypropoxy)-3-methoxybenzaldehyde (11 and 12) and 5-Hydroxy-7-(4-hydroxy-3-methoxyphenyl)-1-[3-methoxy-4-(3-tosyloxypropoxy)phenyl]-1,4,6-heptatrien-3-one (19). To **9**, **10**, or **18** (2.93 mmol) in CH$_3$CN (15 mL) was added silver p-toluenesulfonate (2 g, 7.17 mmol), and the reaction mixtures were stirred under reflux overnight. After removing solvent in vacuo, the resulting residues were extracted with CH$_2$Cl$_2$, washed with water, and dried over Na$_2$SO$_4$. Flash column chromatography (3:1 hexanes−ethyl acetate) gave **11** (680 mg, 66%), **12** (910 mg, 85%), or **19** (1.1 g, 62%) as white solids.

4-(2-Tosyloxyethoxy)-3-methoxybenzaldehyde (11): mp 105.5−107.2 °C; ^{1}H NMR (CDCl$_3$) δ 2.45 (s, 3H), 3.92 (s, 3H), 4.32−4.34 (m, 2H), 4.43−4.45 (m, 2H), 6.93 (d, J = 8.0 Hz, 1H), 7.34 (d, J = 8.0 Hz, 2H), 7.42−7.43 (m, 2H), 7.83 (d, J = 8.5 Hz, 2H), 9.87 (s, 1H); MS (EI) m/z 350 (M$^+$); HRMS calcd for C$_{17}$H$_{18}$O$_6$S, 350.0824; found, 350.0825. Anal. (C$_{17}$H$_{18}$O$_6$S) C, H.

4-(3-Tosyloxypropoxy)-3-methoxybenzaldehyde (12): mp 97.6−98.2 °C; ^{1}H NMR (CDCl$_3$) δ 2.19−2.24 (m, 4H), 2.37 (s, 3H), 3.87 (s, 3H), 4.10 (t, J = 6.0 Hz, 2H), 4.29 (t, J = 6.0 Hz, 2H), 6.88 (d, J = 8.0 Hz, 1H), 7.25 (d, J = 5.0 Hz, 2H), 7.38−7.43 (m, 2H), 7.75 (dd, J = 3.3, 2.0 Hz, 2H), 9.86 (s, 1H); MS (FAB) m/z 387 (M$^+$ + Na); HRMS calcd for C$_{18}$H$_{20}$O$_6$SNa, 387.0878; found, 387.0872. Anal. (C$_{18}$H$_{20}$O$_6$S) C, H.

5-Hydroxy-7-(4-hydroxy-3-methoxyphenyl)-1-[3-methoxy-4-(3-tosyloxypropoxy)phenyl]-1,4,6-heptatrien-3-one (19): ^{1}H NMR (CDCl$_3$) δ 1.21−1.27 (m, 2H), 2.38 (s, 3H), 3.85 (s, 3H), 3.95 (s, 3H), 4.00−4.05 (m, 2H), 4.27−4.32 (m, 2H), 5.82 (s, 1H), 5.86 (s, 1H), 6.49 (dd, J = 16.0, 5.5 Hz, 2H), 6.77 (d, J = 13.5 Hz, 1H), 6.94 (d, J = 8.0 Hz, 1H), 7.02−7.13 (m, 4H), 7.40 (d, J = 9.0 Hz, 2H), 7.59 (d, J = 13.0 Hz, 2H), 7.76 (d, J = 3.5 Hz, 2H); MS (EI) m/z 580 (M$^+$); HRMS calcd for C$_{31}$H$_{32}$O$_9$S, 580.1767; found, 580.1766.

4-(2-Fluoroethoxy)- and 4-(3-Fluoropropoxy)-3-methoxybenzaldehyde (13 and 14). Compound **11** or **12** (0.96 mmol) was dissolved in THF (10 mL), and to this solution was added n-Bu$_4$-NF (1 M in THF, 6 mL, 6 mmol). Reaction mixtures were refluxed for 4 h. After removing solvent in vacuo, products were purified by flash column chromatography (3:1 hexanes−ethyl acetate) to afford **13** (140 mg, 74%), a white solid, or **14** (184.6 mg, 91%), a colorless oil.

4-(2-Fluoroethoxy)-3-methoxybenzaldehyde (13): mp 82.1−84.2 °C; ^{1}H NMR (CDCl$_3$) δ 3.96 (s, 3H), 4.35−4.37 (m, 1H), 4.40−4.42 (m, 1H), 4.79−4.81 (m, 1H), 4.88−4.90 (m, 1H), 7.02 (d, J = 8.0 Hz, 1H), 7.46 (d, J = 8.0 Hz, 2H), 9.89 (s, 1H); MS (EI) m/z 198 (M$^+$); HRMS calcd for C$_{10}$H$_{11}$FO$_3$, 198.0692; found, 198.0691. Anal. (C$_{10}$H$_{11}$FO$_3$) C, H.

4-(3-Fluoropropoxy)-3-methoxybenzaldehyde (14): ^{1}H NMR (CDCl$_3$) δ 2.22−2.32 (m, 2H), 3.93 (s, 3H), 4.25 (t, J = 6.5 Hz, 2H), 4.63 (t, J = 5.5 Hz, 1H), 4.72 (t, J = 5.5 Hz, 1H), 7.00 (d, J = 8.0 Hz, 1H), 7.42−7.45 (m, 2H), 9.86 (s, 1H); MS (EI) m/z 212 (M$^+$); HRMS calcd for C$_{11}$H$_{13}$FO$_3$, 212.0849; found, 212.0850.

4-(3-Methoxyphenyl)-3-buten-2-one Derivatives (1, 2, and 3). 5-Iodovanillin, **13**, or **14** (1.64 mmol) was dissolved in acetone (1 mL) in a pressure tube (ACE glass, 13 × 102 mm). To this solution was carefully added 2.5 M NaOH (1 mL), and the mixture was stirred at room temperature for 24 h. This was then treated with 3 M HCl (5 mL) and then stirred until yellow crystals formed. Products were filtered, washed with water, and then dried. The products, **1** (280.4 mg, 54%), **2** (323.1 mg, 83%), or **3** (280.5 mg, 68%), were obtained as yellow solids after recrystallization from ethanol and water.

4-(4-Hydroxy-3-iodo-5-methoxyphenyl)-3-buten-2-one (1): mp 149.1−151.6 °C; ^{1}H NMR (CD$_3$OD) δ 2.36 (s, 3H), 3.92 (s, 3H), 6.66 (d, J = 16.0 Hz, 1H), 7.23 (d, J = 2.0 Hz, 1H), 7.51 (d, J = 16.0 Hz, 1H), 7.58 (d, J = 1.5 Hz, 1H); MS (EI) m/z 318 (M$^+$); HRMS calcd for C$_{11}$H$_{11}$IO$_3$, 317.9753; found, 317.9751. Anal. (C$_{11}$H$_{11}$IO$_3$) C, H.

4-[4-(2-Fluoroethoxy)-3-methoxyphenyl]-3-buten-2-one (2): mp 109.6−113.9 °C; ^{1}H NMR (CDCl$_3$) δ 3.39 (s, 3H), 3.93 (s, 3H), 4.30 (t, J = 4.5 Hz, 1H), 4.36 (t, J = 4.5 Hz, 1H), 4.77 (t, J = 4.5 Hz, 1H), 4.86 (t, J = 4.5 Hz, 1H), 6.63 (d, J = 16 Hz, 1H), 6.92 (d, J = 8.5 Hz, 1H), 7.10−7.14 (m, 2H), 7.47 (d, J = 16.0 Hz, 1H); MS (EI) m/z 238 (M$^+$); HRMS calcd for C$_{13}$H$_{15}$FO$_3$, 238.1001; found, 238.1001.

4-[4-(3-Fluoropropoxy)-3-methoxyphenyl]-3-buten-2-one (3): mp 73.7−75.2 °C; ^{1}H NMR (CDCl$_3$) δ 2.19−2.26 (m, 1H), 2.26−2.39 (m, 1H), 2.39 (s, 3H), 3.92 (s, 3H), 4.21 (t, J = 6.0 Hz, 2H), 4.64 (t, J = 6.0 Hz, 1H), 4.73 (t, J = 6.0 Hz, 1H), 6.62 (d, J = 16.0 Hz, 1H), 6.92 (d, J = 8.5 Hz, 1H), 7.12 (td, J = 8.5, 2.0 Hz, 2H), 7.48 (d, J = 16.0 Hz, 1H); MS (EI) m/z 252 (M$^+$); HRMS calcd for C$_{14}$H$_{17}$FO$_3$, 252.1162; found, 252.1163.

5-Hydroxy-1-(3-methoxyphenyl)-1,4-hexadien-3-one Derivatives (4, 5, 6, 15, and 16). 2,4-Pentanedione (0.81 mL, 7.92 mmol) and B$_2$O$_3$ (500 mg, 7.18 mmol) were dissolved in ethyl acetate (5 mL), and the solution was stirred at 80 °C for 30 min. To this mixture was added an ethyl acetate solution (10 mL) of the vanillin derivative (**13**, **14**, 5-iodovanillin, vanillin, or 5-bromovanillin (3.6 mmol)) and (n-BuO)$_3$B (0.4 mL, 1.48 mmol). After stirring for 30 min at 80 °C, n-butylamine (0.14 mL, 1.43 mmol) was added dropwise to the mixtures, which were allowed to stir at 100 °C for 1 h. They were then treated with 1 N HCl (10 mL) at 50 °C and stirred at the same temperature for 30 min. Reaction mixtures were extracted with ethyl acetate, washed with water, and then dried over Na$_2$SO$_4$. Flash column chromatography (2:1 hexanes−ethyl acetate), followed by recrystallization from ethanol and water, gave **4** (534.8 mg, 53%), **5** (508.6 mg, 48%), **6** (1.1 g, 85%), **15** (607.2 mg, 72%), or **16** (665.1 mg, 59%) as yellow solids.

1-[4-(2-Fluoroethoxy)-3-methoxyphenyl]-5-hydroxy-1,4-hexadien-3-one (4): mp 105.1−107.1 °C; ^{1}H NMR (CDCl$_3$) δ 2.18 (s, 3H), 3.93 (s, 3H), 4.30 (t, J = 4.5 Hz, 1H), 4.52 (t, J = 4.5 Hz, 1H), 4.76−4.77 (m, 1H), 4.85−4.87 (m, 1H), 5.66 (s, 2H), 6.37 (d, J = 16.5 Hz, 1H), 6.91 (d, J = 4.0 Hz, 1H), 7.10 (td, J = 8.3, 2.0 Hz, 1H), 7.56 (d, J = 15.5 Hz, 1H); MS (EI) m/z 280 (M$^+$); HRMS calcd for C$_{15}$H$_{17}$FO$_4$, 280.1111; found, 280.1112. Anal. (C$_{15}$H$_{17}$FO$_4$) C, H.

1-[4-(3-Fluoropropoxy)-3-methoxyphenyl]-5-hydroxy-1,4-hexadien-3-one (5): mp 70.0−71.2 °C; ^{1}H NMR (CD$_3$Cl) δ 2.18 (s, 3H), 2.22−2.24 (m, 1H), 2.27−2.30 (m, 1H), 3.92 (s, 1H), 4.21 (t,

$J = 6.5$ Hz, 2H), 4.64 (t, $J = 6.0$ Hz, 1H), 4.73 (t, $J = 6.0$ Hz, 1H), 5.66 (s, 2H), 6.36 (d, $J = 15.5$ Hz, 1H), 6.91 (d, $J = 8.5$ Hz, 1H), 7.06–7.12 (m, 2H), 7.56 (d, $J = 15.5$ Hz, 1H); MS (EI) *m/z* 294 (M⁺); HRMS calcd for $C_{16}H_{19}FO_4$, 294.1267; found, 294.1266.

5-Hydroxy-1-(4-hydroxy-3-iodo-5-methoxyphenyl)-1,4-hexadien-3-one (6): mp 178.2–180.0 °C; ¹H NMR (CDCl₃) δ 2.16 (s, 3H), 3.94 (s, 3H), 5.63 (s, 1H), 6.30 (dd, $J = 15.5, 8.0$ Hz, 2H), 6.96 (d, $J = 2.0$ Hz, 1H), 7.43 (d, $J = 15.5$ Hz, 2H), 7.52 (d, $J = 1.5$ Hz, 2H); MS (FAB) *m/z* 361 (M⁺ + H); HRMS calcd for $C_{13}H_{14}IO_4$, 360.9937; found, 360.9937. Anal. ($C_{13}H_{13}IO_4$) C, H.

5-Hydroxy-1-(4-hydroxy-3-methoxyphenyl)-1,4-hexadien-3-one (15): mp 143.5–145.5 °C; ¹H NMR (CDCl₃) δ 2.15 (s, 3H), 3.94 (s, 3H), 5.63 (s, 1H), 5.84 (s, 1H), 6.32 (d, $J = 16.0$ Hz, 1H), 6.93 (d, $J = 15.5$ Hz, 1H), 7.09 (d, $J = 10.5$ Hz, 2H), 7.53 (d, $J = 16.0$ Hz, 1H); MS (EI) *m/z* 234 (M⁺); HRMS calcd for $C_{13}H_{14}O_4$, 234.0892; found, 234.0891.

1-(3-Bromo-4-hydroxy-5-methoxyphenyl)-5-hydroxy-1,4-hexadien-3-one (16): mp 158.8–161.4 °C; ¹H NMR (CDCl₃) δ 1.97 (s, 3H), 3.74 (s, 3H), 6.17 (d, $J = 16.0$ Hz, 1H), 6.80 (d, $J = 2.0$ Hz, 2H), 7.12 (d, $J = 2.0$ Hz, 1H), 7.25 (d, $J = 16.0$ Hz, 2H); MS (FAB) *m/z* 315 (M⁺ + H, ⁸¹Br), 313 (M⁺ + H, ⁷⁹Br); HRMS calcd for $C_{13}H_{14}{}^{81}BrO_4$, 315.0056; found, 315.0048.

5-Hydroxy-1-(4-hydroxy-3-iodo-5-methoxyphenyl)-7-(4-hydroxy-3-methoxyphenyl)-1,4,6-heptatrien-3-one (7) and 1-(3-Bromo-4-hydroxy-5-methoxyphenyl)-5-hydroxy-7-(4-hydroxy-3-methoxyphenyl)-1,4,6-heptatrien-3-one (17). Vanillin (374 g, 2.46 mmol) and B_2O_3 (427 mg, 6.13 mmol) were dissolved in ethyl acetate (5 mL) at 80 °C, and to this mixture was added an ethyl acetate solution (5 mL) of **6** or **16** (3.07 mmol) and (*n*-BuO)₃B (1.65 mL, 6.12 mmol). After stirring for 30 min, mixtures were treated with piperidine (121.7 μL, 1.23 mmol) at 80 °C for 30 min and then with 0.4 N HCl (5 mL) at 50 °C for 30 min. Reaction mixtures were extracted with ethyl acetate, washed with water, and then dried over Na_2SO_4. Flash column chromatography (2:1 hexanes–ethyl acetate) gave **7** (700 mg, 58%) or **17** (549.3 mg, 50%) as orange-colored solids.

5-Hydroxy-1-(4-hydroxy-3-iodo-5-methoxyphenyl)-7-(4-hydroxy-3-methoxyphenyl)-1,4,6-heptatrien-3-one (7): mp 209.9–212.4 °C; ¹H NMR (CD₃OD) δ 3.95 (s, 6H), 5.82 (d, $J = 18.0$ Hz, 2H), 6.48 (d, $J = 15.5$ Hz, 2H), 6.93 (d, $J = 8.0$ Hz, 1H), 7.05 (d, $J = 2.0$ Hz, 2H), 7.12 (dd, $J = 8.0, 2.0$ Hz, 2H), 7.59 (d, $J = 15.5$ Hz, 2H); MS (FAB) *m/z* 495 (M⁺ + H); HRMS calcd for $C_{21}H_{20}IO_6$, 495.0305; found, 495.0312.

1-(3-Bromo-4-hydroxy-5-methoxyphenyl)-5-hydroxy-7-(4-hydroxy-3-methoxyphenyl)-1,4,6-heptatrien-3-one (17): mp 207.6–211.1 °C; ¹H NMR (CD₃OD) δ 3.92 (dd, $J = 7.8, 4.0$ Hz, 6H), 6.53 (dd, $J = 15.5, 1.5$ Hz, 2H), 6.85 (d, $J = 8.0$ Hz, 1H), 7.08 (ddd, $J = 20.0, 10.0, 2.0$ Hz, 3H), 7.34 (d, $J = 2.0$ Hz, 1H), 7.47 (d, $J = 2.0$ Hz, 1H), 7.55 (d, $J = 3.0$ Hz, 2H); MS (FAB) *m/z* 449 (M⁺ + H, ⁸¹Br), 447 (M⁺ + H, ⁷⁹Br); HRMS calcd for $C_{21}H_{20}{}^{81}BrO_6$, 449.0426; found, 449.0421.

1-[4-(3-Fluoropropoxy)-3-methoxyphenyl]-5-hydroxy-7-(4-hydroxy-3-methoxyphenyl)-1,4,6-heptatrien-3-one (8) and 1-[4-(3-Bromopropoxy)-3-methoxyphenyl]-5-hydroxy-7-(4-hydroxy-3-methoxyphenyl)-1,4,6-heptatrien-3-one (18). Compound **15** (337.8 mg, 1.44 mmol) and B_2O_3 (148 mg, 2.13 mmol) were dissolved in ethyl acetate (5 mL) at 80 °C. To this mixture was added an ethyl acetate solution (5 mL) of **10** or **14** (180 mg, 0.85 mmol) and (*n*-BuO)₃B (0.57 mL, 2.11 mmol). After stirring for 30 min, the mixture was treated with piperidine (50 μL, 0.51 mmol) at 80 °C for 30 min, and then with 0.4 N HCl (5 mL) at 50 °C for 30 min. After the reaction mixtures were extracted with ethyl acetate, washed with water, and then dried over Na_2SO_4, the products were purified by flash column chromatography (2:1 hexanes–ethyl acetate) to give **8** (197.4 mg, 54%) or **18** (155.6 mg, 38%) as yellow solids.

In another experiment, **19** (59 mg, 0.10 mmol) was dissolved in THF (5 mL), and to this solution was added *n*-Bu₄NF (1 M in THF, 1 mL, 1.00 mmol). The reaction mixture was refluxed for 4 h, solvent was removed in vacuo, and the product was purified by flash column chromatography (2:1 hexanes–ethyl acetate) to afford **8** (10 mg, 23%) as a yellow solid.

1-[4-(3-Fluoropropoxy)-3-methoxyphenyl]-5-hydroxy-7-(4-hydroxy-3-methoxyphenyl)-1,4,6-heptatrien-3-one (8): mp 92.6–93.2 °C; ¹H NMR (CDCl₃) δ 2.22–2.33 (m, 2H), 3.91 (s, 3H), 3.94 (s, 3H), 4.20 (t, $J = 6.0$ Hz, 2H), 4.62 (t, $J = 5.5$ Hz, 1H), 4.72 (t, $J = 5.5$ Hz, 1H), 5.81 (s, 1H), 6.47 (dd, $J = 15.5, 7.8$ Hz, 2H), 6.93 (dd, $J = 20.0, 9.9$ Hz, 2H), 7.02–7.12 (m, 4H), 7.59 (d, $J = 15.5$ Hz, 2H); MS (EI) *m/z* 428 (M⁺); HRMS calcd for $C_{24}H_{25}FO_6$, 428.1635; found, 428.1638. Anal. ($C_{24}H_{25}FO_6$) C, H.

1-[4-(3-Bromopropoxy)-3-methoxyphenyl]-5-hydroxy-7-(4-hydroxy-3-methoxyphenyl)-1,4,6-heptatrien-3-one (18): ¹H NMR (CDCl₃) δ 2.36–2.41 (m, 2H), 3.62–3.71 (m, 2H), 3.76 (s, 3H), 3.80 (s, 3H), 4.20 (t, $J = 5.5$ Hz, 2H), 5.87 (s, 1H), 5.89 (s, 1H), 6.48 (dd, $J = 15.8, 7.5$ Hz, 2H), 6.87–6.94 (m, 2H), 7.02–7.26 (m, 2H), 7.59 (d, $J = 16.0$ Hz, 2H); MS (EI) *m/z* 490 (M⁺, ⁸¹Br), 488 (M⁺, ⁷⁹Br); HRMS calcd for $C_{24}H_{25}{}^{81}BrO_6$, 490.0818; found, 490.0792.

5-Hydroxy-1-(4-hydroxy-3-methoxy-5-tributylstannylphenyl)-1,4-hexadien-3-one (20) and 5-Hydroxy-7-(4-hydroxy-3-methoxyphenyl)-1-(4-hydroxy-3-methoxy-5-tributylstannylphenyl)-1,4,6-heptatrien-3-one (21). A mixture of the bromo compounds **16** or **17** (0.37 mmol), bis(tributyltin) (1.1 mL, 2.18 mmol), and Pd(Ph₃P)₄ (84.4 mg, 0.037 mmol) in toluene (10 mL) was stirred at 110 °C overnight. At the end of the reactions, solvent was removed in vacuo and the crude products were purified by flash column chromatography (2:1 hexanes–ethyl acetate) to give **20** (38.7 mg, 20%) as an orange-colored oil or **21** (45 mg, 18%) as an orange-colored solid.

5-Hydroxy-1-(4-hydroxy-3-methoxy-5-tributylstannylphenyl)-1,4-hexadien-3-one (20): ¹H NMR (CDCl₃) δ 0.78–0.96 (m, 9H), 1.03–1.19 (m, 6H), 1.26–1.42 (m, 6H), 1.48–1.69 (m, 6H), 2.17 (s, 3H), 3.94 (s, 3H), 5.66 (s, 1H), 5.98 (s, 1H), 6.33 (d, $J = 17.5$ Hz, 1H), 7.01 (d, $J = 2.0$ Hz, 1H), 7.13 (d, $J = 2.0$ Hz, 1H), 7.58 (d, $J = 16.0$ Hz, 1H); MS (FAB) *m/z* 547 (M⁺ + Na); HRMS calcd for $C_{25}H_{40}O_4SnNa$, 547.1851; found, 547.1860.

5-Hydroxy-7-(4-hydroxy-3-methoxyphenyl)-1-(4-hydroxy-3-methoxy-5-tributylstannylphenyl)-1,4,6-heptatrien-3-one (21): mp 95.1–97.5 °C; ¹H NMR (CDCl₃) δ 0.85–0.98 (m, 9H), 1.12–1.47 (m, 18H), 3.94 (d, $J = 8.0$, 6H), 5.91 (s, 2H), 6.46 (d, $J = 16.0$ Hz, 2H), 6.93 (d, $J = 9.5$ Hz, 2H), 7.00–7.14 (m, 2H), 7.52–7.59 (m, 3H), 7.71 (dd, $J = 8.8, 5.0$ Hz, 1H); MS (FAB) *m/z* 659 (M⁺ + H); HRMS calcd for $C_{33}H_{47}O_{26}Sn$, 659.2395; found, 659.2407.

5-Hydroxy-1-(4-hydroxy-3-[¹²⁵I]iodo-5-methoxyphenyl)-1,4-hexadien-3-one([¹²⁵I]6) and 5-Hydroxy-1-(4-hydroxy-3-[¹²⁵I]iodo-5-methoxyphenyl)-7-(4-hydroxy-3-methoxyphenyl)-1,4,6-heptatrien-3-one ([¹²⁵I]7). To 100 μL of the tributylstannyl precursor **20** or **21** (1 mg/mL ethanol) were added 1 N HCl (100 μL) and Na[¹²⁵I]I (185 MBq). Reactions were initiated by adding 100 μL of H_2O_2 (3% w/v) and stirring at room temperature for 10 min. After adding saturated NaHSO₃ (300 μL, aq), radiolabeled products were extracted using ethyl acetate and passed through an anhydrous Na_2SO_4 plug. Solvent was then removed under a gentle stream of N_2, and reaction mixtures were purified by HPLC using a semipreparative column eluted with a 60:40 mixture of CH₃CN and trifluoroacetic acid (0.1%, aq) at a flow rate of 3.0 mL/min. The desired fraction of [¹²⁵I]**6** was eluted between 19 and 20 min, whereas [¹²⁵I]**7** was eluted between 18 and 19 min using a 55:45 mixture of CH₃CN and trifluoroacetic acid (0.1%, aq) at a flow rate of 4.0 mL/min. Specific activities were determined by comparing UV peak areas of the desired radioactive peak and the UV peak areas of different concentrations of unlabeled standard **6** or **7** on HPLC. Aliquots of radioligand ([¹²⁵I]**6** or [¹²⁵I]**7**) were co-injected with unlabeled ligand into the HPLC system to confirm identities.

1-[4-(3-[¹⁸F]Fluoropropoxy)-3-methoxyphenyl]-5-hydroxy-7-(4-hydroxy-3-methoxyphenyl)-1,4,6-heptatrien-3-one ([¹⁸F]8). [¹⁸F]Fluoride (1110 MBq) was placed in a Vacutainer containing *n*-Bu₄NOH (3.2 μL, 4.88 μmol). Three azeotropic distillations were then performed using 100–200 μL aliquots of CH₃CN at 90 °C

(oil bath) under a gentle stream of N_2. The resulting n-Bu$_4$N[^{18}F]F was then dissolved in CH$_3$CN (200 μL) and transferred to a reaction vial containing precursor **12** (2 mg, 5.49 μmol). The reaction mixture was then stirred at 105 °C for 10 min to give [^{18}F]**14**. The resulting mixture was added to an ethyl acetate solution (200 μL) of **15** (2.5 mg, 10.7 μmol) and B$_2$O$_3$ (2 mg, 28.7 μmol), and to this solution were added (n-BuO)$_3$B (10 μL, 37.1 μmol) in ethyl acetate (200 μL) and piperidine (1 μL, 10.1 μmol). This reaction mixture was stirred at 105 °C for 15 min and then treated with 0.4 N HCl (300 μL) at 90 °C for 5 min. The mixture was cooled, diluted with water (2 mL), and extracted with ethyl acetate (2 mL). The organic layer was washed with water and passed through a 3-cm Na$_2$SO$_4$ plug, and solvent was removed under a stream of N$_2$ at 50 °C (water bath). The reaction mixture was then purified by HPLC using a semipreparative column eluted with a 60:40 mixture of CH$_3$CN and trifluoroacetic acid (0.1%, aq) at a flow rate of 3.0 mL/min. The desired product eluted between 23 and 24 min. [^{18}F]**8** was identified and its effective specific activity was determined as described above.

In another experiment, n-Bu$_4$N[^{18}F]F was dissolved in THF (300 μL) and transferred to a reaction vial containing precursor **19** (0.9 mg, 1.45 μmol). The reaction mixture was then stirred at 95 °C for 20 min and passed through a short plug filled with silica gel and Na$_2$SO$_4$ using a 9:1 mixture of CH$_2$Cl$_2$ and CH$_3$OH. The remainder of the procedure was as described above.

Binding Assays Using Aβ(1−40) Aggregates. Aβ(1−40) peptide (0.5 mg) was dissolved in sodium phosphate buffer (10 mM, 1 mL) containing 1 mM EDTA (pH 7.4) and stirred gently at 37 °C for 40−42 h. Binding studies were carried out using the method described in the literature.[14,18] For saturation binding studies, Aβ-(1−40) aggregates (final concentration 20−50 nM) were added to mixtures containing ^{125}I-labeled standard, ^{125}I−IMSB or ^{125}I−IMPY (50 μL, 0.01−8 nM in 40% ethanol). The final concentration of ethanol in a total volume of 1 mL of solution was 10%. Nonspecific binding was determined in the presence of 10 μM CG or thioflavin-T (50 μL in 40% ethanol). For inhibition studies, a total volume of 1 mL containing the ligands (50 μL, 10^{-5}−10^{-10} M in 40% ethanol) and 0.1 nM of radiolabeled standard (50 μL in 40% ethanol) was used. Reaction mixtures were incubated with shaking at room temperature for 3 h, and bound radioactivity was collected on Whatman GF/B filters using a cell harvester (Inotech Biosystems, Dottikon, Switzerland) and washed twice using 3 mL of 10% ethanol. The filters containing radioactivity were then counted using a gamma counter at a counting efficiency of 83%. Data were analyzed using software Prism, and K_d and K_i values were calculated.

Partition Coefficient Measurement. Radioligands, [^{125}I]**6**, [^{125}I]-**7**, or [^{18}F]**8**, collected from HPLC, were concentrated under a gentle stream of N$_2$ and redissolved in 10% ethanol−saline. The radioligands were respectively added to premixed suspensions containing 600 μL octanol and 600 μL water and then vortexed vigorously for 3 min and centrifuged at 2000 rpm for 5 min. Two layers separated out, and 100 μL aliquots of the octanol and aqueous layers were removed and counted. Samples from the octanol and aqueous layers were repartitioned until consistent values were obtained. The experiments were carried out in triplicate. Log $P_{o/w}$ was expressed as the logarithm of the ratio of the counts per minute from octanol versus that of water.[39]

Metabolism Studies. Mice (ICR, male 25−30 g) were injected with [^{18}F]**8** (14.8 MBq/mouse) via a tail vein and sacrificed at 2, 30, and 60 min post-iv-injection. At the designated time points, samples of blood and whole brain were collected, homogenized in 1 mL of chilled absolute ethanol, and centrifuged at 3000 rpm for 3 min. Supernatants were analyzed by radio-TLC using a 20:1 mixture of CH$_2$Cl$_2$−CH$_3$OH and a 1:1:0.01 mixture of CH$_2$Cl$_2$−CH$_3$OH−triethylamine.

Biodistribution in Normal Mice. ICR mice (male, 25−30 g, four mice per time point) were injected with [^{125}I]**6** (0.74 MBq) or [^{18}F]**8** (1.85 MBq) in 0.2 mL of 10% ethanol−saline via a tail vein. The mice were sacrificed at the indicated times (2, 30, 60, and 120 min). Samples of blood, heart, lung, liver, spleen, kidney, muscle,

brain, and thyroid (or bone) were removed, weighed, and counted. Data are expressed as the percent injected dose per gram of tissue (% ID/g).

In another experiment, mice were injected with a mixture of radioligand [^{18}F]**8** and piperine (2 mg/kg) in 0.2 mL of 10% ethanol−saline via a tail vein. The remainder of the procedure was as described above.

References

(1) Ginsberg, S. D.; Schmidt, M. L.; Crino, P. B.; Eberwine, J. H.; Lee, V. M. Y.; Trojanowski, J. Q. Molecular Pathology of Alzheimer's Disease and Related Disorders. In *Cerebral Cortex: Neurodegenerative and Age-Related Changes in Structure and Function of Cerebral Cortex*; Peters, A., Morrison, J. H., Eds.; Kluwer Academic/Plenum: New York, 1999; pp 603−654.

(2) Lee, V. M.; Trojanowski, J. Q. Neurodegenerative Tauopathies: Human Disease and Transgenic Mouse Models. *Neuron* **1999**, *24*, 507−510.

(3) Selkoe, D. J. The Origins of Alzheimer Disease: A is for Amyloid. *JAMA* **2000**, *283*, 1615−1617.

(4) Mathis, C. A.; Wang, Y.; Klunk, W. E. Imaging β-Amyloid Plaques and Neurofibrillary Tangles in the Aging Human Brain. *Curr. Pharm. Design* **2004**, *10*, 1469−1492.

(5) Tubis, M.; Blahd, W. H.; Nordyke, R. A. The Preparation and Use of Radioiodinated Congo Red in Detecting Amyloidosis. *J. Am. Pharm. Assoc.* **1960**, *49*, 422−425.

(6) Mathis, C. A.; Mahmood, K.; Debnath, M. L.; Klunk, W. E. Synthesis of a Lipophilic, Radioiodinated Ligand with High Affinity to Amyloid Protein in Alzheimer's Disease Brain Tissue. *J. Labelled Compd. Radiopharm.* **1997**, *40*, 94−95.

(7) Dezutter, N. A.; De Groot, T. J.; Busson, R. H.; Janssen, G. A.; Verbruggen, A. M. Preparation of ^{99m}Tc-N$_2$S$_2$ Conjugates of Chrysamine G, Potential Probes for the beta-Amyloid Protein of Alzheimer's Disease. *J. Labelled Compd. Radiopharm.* **1999**, *42*, 309−324.

(8) Dezutter, N. A.; Dom, R. J.; De Groot, T. J.; Bormans, G. M.; Verbruggen, A. M. ^{99m}Tc-MAMA-Chrysamine G, a Probe for β-Amyloid Protein of Alzheimer's Disease. *Eur. J. Nucl. Med.* **1999**, *26*, 1392−1399.

(9) Han, H.; Cho, C. G.; Lansbury, P. T. Technetium Complexes for the Quantitation of Brain Amyloid. *J. Am. Chem. Soc.* **1996**, *118*, 4506−4507.

(10) Zhen, W.; Han, H.; Anguiano, M.; Lemere, C. A.; Cho, C. G.; Lansbury, P. T. Synthesis and Amyloid Binding Properties of Rhenium Complexes: Preliminary Progress Toward a Reagent for SPECT Imaging of Alzheimer's disease Brain. *J. Med. Chem.* **1999**, *42*, 2805−2815.

(11) Levin, V. A. Relationship of Octanol/Water Partition Coefficient and Molecular Weight to Rat Brain Capillary Permeability. *J. Med. Chem.* **1980**, *23*, 682−684.

(12) Abraham M. H. The Factors that Influence Permeation Across the Blood-Brain Barrior. *Eur. J. Med. Chem.* **2004**, *39*, 235−240.

(13) Styren, S. D.; Hamilton, R. L.; Styren, G. C.; Klunk, W. E. X-34, a Fluorescent Derivatie of Congo Red: a Novel Histochemical Stain for Alzheimer's Disease Pathology. *J. Histochem. Cytochem.* **2000**, *48*, 1223−1232.

(14) Skovronsky, D. M.; Zhang, B.; Kung, M. P.; Kung, H. F.; Trojanowski, J. Q.; Lee, V. M. Y. In Vivo Detection of Amyloid Plaques in a Mouse Model of Alzheimer's Disease. *Proc. Natl. Acad. Sci. U.S.A.* **2000**, *97*, 7609−7614.

(15) Zhuang, Z. P.; Kung, M. P.; Hou, C.; Skovronsky, D. M.; Gur, T. L.; Trojanowski, J. Q.; Lee, V. M. Y.; Kung, H. F. Radioiodinated Styrylbenzenes and Thioflavins as Probes for Amyloid Aggregates. *J. Med. Chem.* **2001**, *44*, 1905−1914.

(16) Agdeppa, E. D.; Kepe, V.; Liu, J.; Flores-Torres, S.; Satyamurthy, N.; Petric, A.; Cole, G. M.; Small, G. W.; Huang, S. C.; Barrio, J. R. Binding Characteristics of Radiofluorinated 6-Dialkylamino-2-Naphthaylethylidene Derivatives as Positron Emission Tomography Imaging Probes of β-Amyloid Plaques in Alzheimer's Disease. *J. Neurosci.* **2001**, *21*, RC189.

(17) Barrio, J. R.; Huang, S. C.; Cole, G.; Satyamurthy, N.; Petric, A.; Phelps, M. E.; Small, G. PET Imaging of Tangles and Plaques in Alzheimer Disease with a Highly Hydrophobic Probe. *J. Labelled Compd. Radiopharm.* **1999**, *42*, S194−195.

(18) Klunk, W. E.; Wang, Y.; Huang, G.; Debnath, M. L.; Holt, D. P.; Mathis, C. A. Uncharged Thioflavin-T Derivatives Bind to Amyloid-Beta Protein with High Affinity and Readily Enter the Brain. *Life Sci.* **2001**, *69*, 1471−1484.

(19) Mathis, C. A.; Bacskai, B. J.; Kajdasz, S. T.; McLellan, M. E.; Frosch, M. P.; Hyman, B. T.; Holt, D. P.; Wang, Y.; Huang, G.-F.; Debnath, M. L.; Klunk, W. E. A Lipophilic Thioflavin-T Derivative for Positron Emission Tomography (PET) Imaging of Amyloid in Brain. *Bioorg. Med. Chem. Lett.* **2002**, *12*, 295−298.

(20) Zhuang, Z.-P.; Kung, M. P.; Hou, C.; Plössl, K.; Skovronsky, D.; Gur, T. L.; Trojanowski, J. Q.; Lee, V. M. Y.; Kung, H. F. IBOX (2-(4′-dimethylaminophenyl)-6-iodobenzoxazole): A Ligand for Imaging Amyloid Plaques in the Brain. *Nucl. Med. Biol.* **2001**, *28*, 887−894.

(21) Zhuang, Z. P.; Kung, M. P.; Wilson, A.; Lee, C. H.; Plössl, K.; Hou, C.; Holtzman, D. M.; Kung, H. F. Structure−Activity Relationship of Imidazo[1,2-a]pyridines as Ligands for Detecting β-Amyloid Plaques in the Brain. *J. Med. Chem.* **2003**, *46*, 237−243.

(22) Mathis, C. A.; Wang, Y.; Holt, D. P.; Huang, G. F.; Debnath, M. L.; Klunk, W. E. Synthesis and Evaluation of ¹¹C-Labeled 6-Substituted 2-Arybenzothiazoles as Amyloid Imaging Agents. *J. Med. Chem.* **2003**, *46*, 2740−2754.

(23) Ono, M.; Kung, M. P.; Hou, C.; Kung, H. F. Benzofuran Derivatives as Aβ-aggregate-specific Imaging Agents for Alzheimer's disease. *Nucl. Med. Biol.* **2002**, *29*, 633−642.

(24) Kung, M. P.; Hou, C. H.; Zhuang, Z. P.; Cross, A. J.; Maier, D. L.; Kung, H. F. Characterization of IMPY as a Potential Imaging Agent for β-Amyloid Plaques in Double Transgenic PSAPP Mice. *Eur. J. Nucl. Med. Mol. Imaging* **2004**, *31*, 1136−1145.

(25) Kung, M. P.; Hou, C. H.; Zhuang, Z. P.; Skovronsky, D.; Kung, H. F. Binding of Two Potential Imaging Agents Targeting Amyloid Plaques in Postmortem Brain Tissues of Patients with Alzheimer's Disease. *Brain Res.* **2004**, *1025*, 98−105.

(26) Engler, H.; Blomqvist, G.; Bergstrom, M.; Estrada, S.; Sandell, J.; Antoni, G.; Långström B.; Barletta, J.; Klunk, W.; Debnath, M.; Holt, D.; Wang, Y.; Huang, G. F.; Mathis, C. First Human Study with a Benzothiazole Amyloid-Imaging Agent in Alzheimer's Disease and Control Subjects. *Neurobiol. Aging* **2002**, *23*, S429.

(27) Klunk, W. E.; Engler, H.; Nordberg, A.; Wang, Y.; Blomqvist, G.; Holt, D. P.; Bergström, M.; Savitcheva, I.; Huang, G. F.; Estrada, S.; Ausén, B.; Debnath, M. L.; Barletta, J.; Price, J. C.; Sandell, J.; Lopresti, B. J.; Wall, A.; Koivisto, P.; Antoni, G.; Mathis, C. A.; Långström B. Imaging Brain Amyloid in Alzheimer's Disease with Pittsburgh Compound-B. *Ann. Neurol.* **2004**, *55*, 306−319.

(28) Ono, M.; Wilson, A.; Nobrega, J.; Westaway, D.; Verhoeff, P.; Zhuang, Z. P.; Kung, M. P.; Kung, H. F. ¹¹C-Labeled Stilbene Derivatives as Aβ-aggregate-specific PET Imaging Agents for Alzheimer's Disease. *Nucl. Med. Biol.* **2003**, *30*, 565−571.

(29) Cheng, A. L.; Hsu, C. H.; Lin, J. K.; Hsu, M. M.; Ho, Y. F.; Shen, T. S.; Ko, J. Y.; Lin, J. T.; Lin, B. R.; Ming-Shiang, W.; Yu, H. S.; Jee, S. H.; Chen, G. S.; Chen, T. M.; Chen, C. A.; Lai, M. K.; Pu, Y. S.; Pan, M. H.; Wang, Y. J.; Tsai, C. C.; Hsieh, C. Y. Phase I Clinical Trial of Curcumin, a Chemopreventive Agent, in Patients with High-Risk or Pre-Malignant Lesions. *Anticancer Res.* **2001**, *21*, 2895−2900.

(30) Lin, J. K.; Shih, C. A. Inhibitory Effect of Curcumin on Xanthine Dehydrogenase/oxidase Induced by Phorbol-12-myristate-13acetate in NIH3T3 cells. *Carcinogenesis* **1994**, *15*, 1717−1721.

(31) Chan, M. M.; Huang, H. I.; Fenton, M. R.; Fong, D. In Vivo Inhibition of Nitric Oxide Synthase Gene Expression by Curcumin, a Cancer Preventive Natural Product with Anti-inflammatory Properties. *Biochem. Pharmacol.* **1998**, *55*, 1955−1962.

(32) Ganguli, M.; Chandra, V.; Kamboh, M. I.; Johnston, J. M. Apolipoprotein E Polymorphism and Alzheimer Disease: The Indo-US Cross-National Dementia Study. *Arch. Neurol.* **2000**, *57*, 824−830.

(33) Lim, G. P.; Chu, T.; Yang, F.; Beech, W.; Frautschy, S. A.; Cole, G. M. The Curry Spice Curcumin Reduces Oxidative Damage and Amyloid Pathology in an Alzheimer Transgenic Mouse. *J. Neurosci.* **2001**, *21*, 8370−8377.

(34) Yang, F.; Lim, G. P.; Befum, A. N.; Ubeda, O. J.; Simmons, M. R.; Ambegaokar, S. S.; Chen, P.; Kayed, R.; Glabe, C. G.; Frautschy, S. A.; Cole, G. M. Curcumin Inhibits Formation of Amyloid β Oligomers and Fibrils, Binds Plaques, and Reduces Amyloid in Vivo. *J. Biol. Chem.* **2005**, *280*, 5892−5901.

(35) Kikuzaki, H.; Nakatani, N. Antioxidant Effect of Some Ginger Constituents. *J. Food Sci.* **1993**, *58*, 1407−1410.

(36) Smith, L. R. Rheosmin ("Raspberry Ketone") and Zingerone, and Their Preparation by Crossed Aldol-Catalytic Hydrogenation Sequences. *Chem. Educ.* **1996**, *1*, 1−18.

(37) Masuda, T.; Matsumura H.; Oyama, Y.; Takeda, Y.; Jitoe, A.; Kida, A.; Hidaka, K. Synthesis of (±)-Cassumunins A and B, New Curcuminoid Antioxidants Having Protective Activity of the Living Cell Against Oxidant Damage. *J. Nat. Prod.* **1998**, *61*, 609−613.

(38) Shoba, G.; Joy, D.; Joseph, T.; Majeed, M.; Rajendran, R.; Srinivas P. S. Influence of Piperine on the Pharmacokinetics of Curcumin in Animals and Human Volunteers. *Planta Med.* **1998**, *64*, 353−356.

(39) Li, H.; Gildehaus, F. J.; Dresel, S.; Patt, J. T.; Shen, M.; Zhu, T.; Liu, B.; Tang, Z.; Tatsch, K.; Hahn, K. Comparison of In Vivo Dopamine D₂ Receptor Binding of [¹²³I]AIBZM and [¹²³I]IBZM in Rat Brain. *Nucl. Med. Biol.* **2001**, *28*, 383−389.